Testing neutrino spectra formation in collapsing stars with the diffuse supernova neutrino flux

Cecilia Lunardini*

Institute for Nuclear Theory and Department of Physics, University of Washington, Seattle, Washington 98195, USA

(Received 31 January 2007; published 27 April 2007)

I address the question of what can be learned from the observation of the diffuse supernova neutrino flux in the precision phase, at next generation detectors of Megaton scale. An analytical study of the spectrum of the diffuse flux shows that, above realistic detection thresholds of 10 MeV or higher, the spectrum essentially reflects the exponential-times-polynomial structure of the original neutrino spectrum at the emission point. There is only a weak (tens of percent) dependence on the power β describing the growth of the supernova rate with the redshift. Different original neutrino spectra correspond to large differences in the observed spectrum of events at a water Cherenkov detector: for typical supernova rates, the ratio of the numbers of events in the first and second energy bins (of 5 MeV width) varies in the interval 1.5–4.3 for pure water (energy threshold 18 MeV) and in the range 1–2.5 for water with gadolinium (10 MeV threshold). In the first case, discrimination would be difficult due to the large errors associated with background. With gadolinium, instead, the reduction of the total error down to the 10%–20% level would allow spectral sensitivity, with a dramatic improvement of precision with respect to the SN1987A data. Even in this latter case, for typical neutrino luminosity the dependence on β is below sensitivity, so that it can be safely neglected in data analysis.

DOI: 10.1103/PhysRevD.75.073022 PACS numbers: 97.60.Bw, 14.60.Pq

I. INTRODUCTION

Almost 20 years after the detection of neutrinos from SN1987A, there is a hunger for new neutrino data from supernovae, which are needed to advance our understanding of the physics of core collapse, and are precious to improve our knowledge of neutrino physics.

Considering how rare supernovae are in our immediate galactic neighborhood [1,2], it is likely that the next supernova neutrino data will come to us not in the form of a high statistics signal from a nearby star, but as a diffuse flux of neutrinos from all the supernovae in the sky, each of them too far to give a significant signal.

There are reasons to believe that the detection of this diffuse supernova neutrino flux (DSNνF) may soon be a reality. Indeed, the Super-Kamiokande (SK) experiment has already obtained an upper bound on this flux within an order of magnitude of the theoretical predictions: 1.2 electron antineutrinos ($\bar{\nu}_e$) $s^{-1}\,cm^{-2}$ [3] (see also [4–6] for other, less constraining, experimental results). The sensitivity of SK will increase substantially in the next 5–10 years with the gadolinium addition, GADZOOKS [7]. In this new configuration, the rate of events due to the DSNνF could reach $\mathcal{O}(1)$ events/year, which implies the possibility to obtain the very first detection of the diffuse flux. If the supernova rate is precisely known, GADZOOKS could also give information on the neutrino spectrum at least for part of the parameter space, with sensitivity comparable to that of the SN1987A data [8].

After SK and GADZOOKS, a new generation of detectors with larger volumes will become operational. Some projects will require ~1 Megaton (Mton) water volumes (HyperKamiokande, UNO, MEMPHYS [9–11]), while other ideas involve a 50 kt mass of liquid scintillator (LENA, [12,13]) and 100 kt-scale liquid argon detectors [14,15]. For values of the DSNνF that are considered typical, these new detectors are expected to accumulate a statistics of several tens or even hundreds of events from the DSNνF in the space of few years running time.

It is clear, thus, that the advent of these new detectors will make it possible to go beyond the phase of discovery and start a phase of detailed study of the diffuse flux. The number of events, their energy spectrum, and their spatial and temporal distributions will be analyzed in depth to study the neutrino emission from a supernova, the local and cosmological supernova rate, neutrino oscillations, and possible exotic particle physics affecting neutrinos.

The question of what will be possible to learn from the DSNνF data in the precision phase, and how well, has received only limited attention. An initial study by Yuksel, Ando, and Beacom [8] considered specific examples, focusing on the low statistics of GADZOOKS. The main result was that GADZOOKS has a chance to test the neutrino spectrum if the flux is close to the current Super-Kamiokande limit. The status of the art on what the data from the DSNνF will tell us is well summarized in the work by Fogli *et al.* [16], where a detailed study of the background is presented for detection with pure water and with water with gadolinium.

In this paper I expand on previous works by discussing in detail what can be learned from the *energy spectrum* of the data from the diffuse flux, focusing on Megaton scale detectors. The energy distribution of events depends on the spectrum of the neutrinos emitted by an individual supernova and therefore its study would be a crucial test of models of neutrino transport inside the collapsed matter

*Electronic address: lunardi@phys.washington.edu

of a supernova, as well as of neutrino oscillations inside the star. The observed energy spectrum also depends on the distribution of supernovae with the redshift, i.e. on the dependence of the supernova rate with the distance (or, equivalently, time from the big bang). Indeed, the larger the fraction of supernovae at cosmological distance, the softer the DSNνF spectrum is, due to the effect of redshift of energy. To get information on the evolution of the supernova rate with the cosmological time from the diffuse neutrinos would be of extreme interest.

Here I present an analytical study of the DSNνF spectrum as well as numerical results for the spectrum of $\bar{\nu}_e$-induced events at a Megaton water Cherenkov detector. The analytics offers insight on the numerical findings. Of both the DSNνF spectrum and the observed signal, I examine the dependencies on the power of evolution of the supernova rate with the distance and on the average energy and spectral shape of the neutrino flux at the source. I also give typical numbers of events and discuss the sensitivity of specific observables to the neutrino spectrum, considering the errors associated with the background and possible uncertainties on the supernova rate normalization.

The paper opens with generalities (Sec. II), followed by the analytical study of the DSNνF spectrum in Sec. III. The observable signal is discussed in Sec. IV. A summary and discussion close the paper in Sec. V.

II. GENERALITIES

A core collapse supernova is an extremely powerful neutrino source, releasing about 3×10^{53} ergs of energy within $\sim$10 seconds in neutrinos and antineutrinos of all flavors. The spectrum of these neutrinos is approximately thermal, with average energies in the range of 10–20 MeV and with the muon and tau species being harder than the electron ones due to their weaker (neutral current only) coupling to matter. Inside the star, the neutrinos undergo either partial or total flavor conversion depending on the mixing angle θ_{13} and on the mass hierarchy (ordering) of the neutrino mass spectrum (see, e.g., [17,18]). For definiteness, here I focus on the $\bar{\nu}_e$ species, as it is the most relevant for detection (see Sec. IV).

The energy spectrum of $\bar{\nu}_e$ as they exit the star can be described as [19]

$$\frac{dN}{dE} \simeq \frac{(1+\alpha)^{1+\alpha} L}{\Gamma(1+\alpha) E_0^2} \left(\frac{E}{E_0}\right)^{\alpha} e^{-(1+\alpha)E/E_0}, \qquad (1)$$

where $E_0 \sim$ 9–20 MeV is the average energy and L the (time-integrated) luminosity in $\bar{\nu}_e$, $L \sim 5 \times 10^{52}$ ergs. α is a parameter describing the shape of the spectrum, $\alpha \simeq$ 2–5 [19], with larger α corresponding to a narrower spectrum. The form (1) is justified by a number of arguments. First, it is a good fit to numerical calculations of neutrino transport before flavor conversion. Given this, Eq. (1) also describes the $\bar{\nu}_e$ spectrum *after* conversion if the conversion is total, which happens for inverted mass hierarchy and $\sin^2\theta_{13} \gtrsim 10^{-4}$ [17,18], or if the $\bar{\nu}_e$ and $\bar{\nu}_\mu$, $\bar{\nu}_\tau$ original spectra are very similar. This is favored by the recent finding that the $\bar{\nu}_e$ and $\bar{\nu}_\mu$, $\bar{\nu}_\tau$ average energies may differ only by 10%–20% [19]. If the conversion of $\bar{\nu}_e$ is partial and the hierarchy between the electron and nonelectron original spectra is strong, Eq. (1) is still an accurate description of the neutrino spectrum above its average energy, where the flux is dominated by the harder component from oscillated muon and tau neutrinos [18]. This condition is met above the realistic detection thresholds of $\sim$10–20 MeV energy, since the DSNνF average energy is typically smaller than $\sim$5–6 MeV (see Fig. 1).

I have estimated the error associated with approximating a composite spectrum with the form (1), in the case of maximal permutation of the neutrino fluxes, which is realized (for antineutrinos, of interest here) for the normal mass hierarchy, or for the inverted hierarchy with $\sin^2\theta_{13} \lesssim 3 \times 10^{-6}$ [17,18]. I assumed a difference in the $\bar{\nu}_e$ and $\bar{\nu}_\mu$, $\bar{\nu}_\tau$ average energies up to 30%, and up to a factor of 2 difference in the luminosities of the electron and nonelectron flavors. The result is that the error is smaller than 6% above 10 MeV of energy, if Eq. (1) is used with L and E_0 being the luminosity and the average energy of the composite spectrum, and α chosen to reproduce the width of the composite spectrum.

Finally, the form (1) is supported, as a phenomenological description, by the fact that it fits well the data from SN1987A [20].

Given the neutrino output of an individual supernova, one has to sum over the supernova population of the universe. This is described by the cosmological rate of supernovae, $R_{SN}(z)$, defined as the number of supernovae in the unit time per unit of comoving volume at redshift z. Its value today ($z = 0$) is estimated in the range of

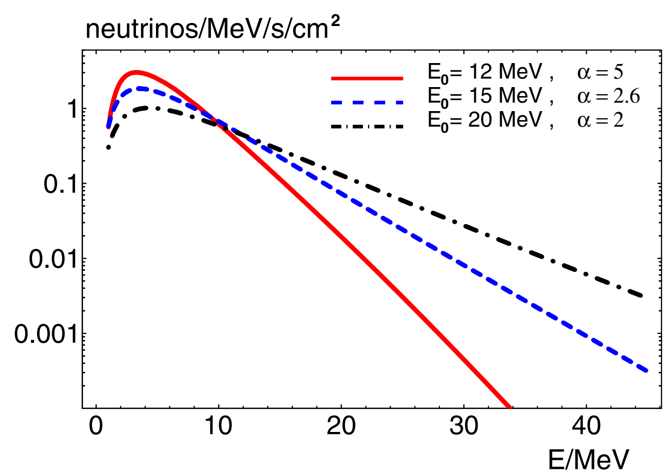

FIG. 1 (color online). Examples of spectra of the diffuse supernova neutrino flux for different original neutrino spectra and a fixed supernova rate. For the latter, I used the parameters $\beta = 3.28$, $R_{SN}(0) = 10^{-4}$ Mpc^{-3} yr^{-1}. The luminosity $L = 5 \times 10^{52}$ ergs [see Eq. (1)] was adopted.

$R_{SN}(0) \sim 10^{-4}$ Mpc^{-3} yr^{-1}, with uncertainty of a factor of 2 or so [21,22] due to finite statistics and uncertain systematic errors due to dust extinction. Theory [23] and data indicate (see e.g. [22]) that after the beginning of star formation the supernova rate (SNR from here on) was first somewhat constant in time, and then decreased after the redshift dropped below $z \sim 1$. It can be described phenomenologically with a broken power law:

$$R_{SN}(z) = R_{SN}(0)(1+z)^{\beta} \quad \text{for } z \leq 1$$
$$= R_{SN}(0)2^{\beta} \quad \text{for } z > 1, \tag{2}$$

where β is in the range $\beta \sim 2$–5 from the statistical analysis of supernova observational data only [21]. It becomes more constrained around $\beta \sim 3$ (best fit value $\beta = 3.28$) if the more precise (but only indirectly related to the SNR; see [21,24]) measurements of the star formation rate are used instead [22]. Here I will consider the wider interval $\beta \sim 2$–5 to be conservative.

Using the supernova rate R_{SN} and the individual neutrino flux dN/dE, one finds the diffuse flux, differential in energy:

$$\Phi(E) = \frac{c}{H_0} \int_0^{z_{max}} R_{SN}(z) \frac{dN(E')}{dE'} \frac{dz}{\sqrt{\Omega_m(1+z)^3 + \Omega_\Lambda}}, \tag{3}$$

(see e.g. [24]). Here E and $E' = (1+z)E$ are the neutrino energy at Earth and at the production point; $\Omega_m \simeq 0.3$ and $\Omega_\Lambda \simeq 0.7$ are the fraction of the cosmic energy density in matter and dark energy, respectively; c is the speed of light; and H_0 is the Hubble constant. The maximum redshift z_{max} accounts for the expected decrease of the SNR with z beyond $z \sim 5$ or so. The dependence of the DSNνF above realistic detection thresholds on z_{max} is weak due to the effect of redshift. I will use $z_{max} = 5$ from here on.

Throughout the paper, the expression (3) will be used for the DSNνF. This formula is valid in the continuum limit, and only if individual variations between different stars are negligible. This last statement has not been checked in detail; it is however supported by the results of numerical simulations [25].

From Eqs. (1)–(3) one sees that the spectrum of the DSNνF depends on three variables: α, E_0, and β, i.e. on the spectrum of the neutrinos emitted by an individual star ("original neutrino spectrum" from here on) and on the power of growth of the SNR with z. Figure 1 shows the DSNνF spectrum from Eq. (3) for different original neutrino spectra; in this figure L, $R_{SN}(0)$, and β are held fixed while α and E_0 are varied (see caption for details) to show how the slope of the spectrum can change. Specifically, the spectrum is steeper for smaller E_0 and larger α, as it will be discussed in detail in Sec. III.

III. THE ENERGY SPECTRUM OF THE DIFFUSE FLUX

What is the energy distribution of the diffuse supernova neutrinos? How is it related to the original neutrino spectrum and to the cosmological distribution of supernovae? In the light of what was discussed in Sec. II, the answer is only partially intuitive. Because of the redshift of energy, the farther a supernova is from us the more its contribution is shifted to lower energy. This means that the DSNνF does not retain the same spectrum that the neutrinos had at emission, but have instead a distorted—and overall softer—distribution with respect to it, which depends on the SNR. One expects the largest distortion in the lowest energy part of the spectrum, $E \sim 5$–10 MeV, where the contribution of high redshift supernovae is larger. In contrast, in the high energy end of the DSNνF spectrum, $E \gtrsim 15$–20 MeV, the flux is largely dominated by stars with negligibly small redshift, and therefore it should be closer to the original spectrum.

Let us see this in a more quantitative way, by examining the spectrum that results from Eq. (3). There, the integration cannot be done exactly. Still, however, one can find useful analytical approximations that help to understand the energy dependence of the DSNνF. Considering that current and planned searches of the diffuse flux have thresholds of $\sim$10 MeV or higher, it is sensible to focus on the high end of the spectrum, i.e. on the small redshift approximation, $z \ll 1$. In this limit one can make the following simplifications:

(1) The substitution

$$[\Omega_m(1+z)^3 + \Omega_\Lambda]^{-1/2} \longrightarrow (1+z)^{-(3/2)\Omega_m}. \tag{4}$$

The two expressions coincide at first order in z under the condition that $\Omega_m + \Omega_\Lambda = 1$, which is favored by current cosmological data.

(2) Neglect the contribution of the supernovae beyond the $z \simeq 1$ break of the SNR, specifically

$$R_{SN}(z) = R_{SN}(0)(1+z)^{\beta} \quad \text{for } z \lesssim z_{max},$$
$$= 0 \quad \text{for } z > z_{max}, \tag{5}$$

with $z_{max} = 1$.

With these approximations, the integral in Eq. (3) gives the following result:

$$\Phi_e \simeq R_{SN}(0) \frac{c}{H_0} \frac{L}{\Gamma(2+\alpha)\epsilon^2} \left(\frac{E}{\epsilon}\right)^{\alpha-\eta-1} (\Gamma[\eta+1, E/\epsilon] - \Gamma[\eta+1, (1+z_{max})E/\epsilon]), \tag{6}$$

where I define $\eta \equiv \alpha + \beta - 3\Omega_m/2$ and $\epsilon = E_0/(1+\alpha)$ for brevity. Considering $\alpha \gtrsim 2$ (Sec. II), we have $\epsilon \lesssim E_0/3$.

It is possible to further simplify the result by dropping the contribution of the upper limit of integration $(1 + z_{max})E/\epsilon$, which at high energy is exponentially suppressed with respect to the term due to the lower limit.

Furthermore, if η is an integer, one can also use the expression of the Γ function in terms of an exponential times a polynomial [26], and get

$$\Phi_e \simeq R_{\rm SN}(0)\frac{c}{H_0}\frac{L}{\Gamma(2+\alpha)\epsilon^2}e^{-(E/\epsilon)} \times \sum_{k=0}^{\eta}\left[\left(\frac{E}{\epsilon}\right)^{\alpha-1-k}\frac{\eta!}{(\eta-k)!}\right], \tag{7}$$

or, explicitly,

$$\Phi_e \simeq R_{\rm SN}(0)\frac{c}{H_0}\frac{L}{\Gamma(2+\alpha)\epsilon^2}e^{-(E/\epsilon)}\left[\left(\frac{E}{\epsilon}\right)^{\alpha-1} + \eta\left(\frac{E}{\epsilon}\right)^{\alpha-2} + \eta(\eta-1)\left(\frac{E}{\epsilon}\right)^{\alpha-3} + \eta(\eta-1)(\eta-2)\left(\frac{E}{\epsilon}\right)^{\alpha-4} + \ldots\right]. \tag{8}$$

Equation (8) turns out to be numerically accurate also for noninteger η, provided that the sum is truncated at the integer nearest to η. It also has the advantage of simplicity, so it can be used to understand the physics.

Let us pause for a moment and study the result (8). This expression tells us that the DSNνF spectrum is similar to the original spectrum in the general structure of an exponential times a polynomial part. More specifically, the term $e^{-E/\epsilon}/\epsilon^2$ in Eq. (8) is the same as in the original spectrum, while the polynomial part is more complicated and contains the information on the cosmology (i.e., on β and on Ω_m), through the quantity η. The latter enters the result only in the coefficients of the various powers of energy, a very weak dependence with respect to the exponential decay of the spectrum in E/ϵ. Notice that, in agreement with intuition, the dependence on η becomes weaker for higher energy: indeed, in the limit $E \gg \epsilon$, the polynomial part is dominated by the η-independent term $(E/\epsilon)^{\alpha-1}$. In general, Eq. (8) suggests that the exponential captures most of the energy dependence, with only slower variations due to the polynomial part. Thus, one can consider fitting the DSNνF spectrum at high energy with a simple exponential form, as already suggested in [27]:

$$\Phi_e = \Phi_e(0)e^{-E/\langle E\rangle}. \tag{9}$$

I find that, as expected, $\langle E\rangle$ is numerically close to ϵ, with differences smaller than $\sim$30%.

Figure 2 compares the exact spectrum (see caption for details), calculated numerically, with the three approximations: the sophisticated one, Eq. (6); the cruder one, Eq. (7); and the phenomenological one, Eq. (9). For the latter, the parameters $\langle E\rangle$ and $\Phi_e(0)$ have been adjusted to fit the numerical curve in the interval $E \simeq 20$–30 MeV. The figure shows that the sophisticated result, Eq. (6), underestimates the flux at low energy as a result of neglecting the $z > 1$ part of the SNR. Instead, the cruder description, Eq. (7), overestimates the flux at low energy due to dropping the (negative) contribution of the upper limit of integration in (6), which is equivalent to taking the SNR as growing with constant power all the way to $z \to \infty$. The simple fitted exponential form lies between the two approximations and works surprisingly well down to $E \sim$ 5–6 MeV, probably because by fitting $\langle E\rangle$ one effectively reproduces at least part of the contributions that are not included in the forms (6) and (7), especially the $z > 1$ part of the SNR.

I have studied the precision of Eqs. (6) and (7) in detail. First, I fixed $\beta = 3.28$ and varied the neutrino spectral parameters in the intervals $\alpha = 2$–5 and $E_0 =$ 9–18 MeV. I obtained that the full result, Eq. (6), is precise to better than 12% (40%) at $E = 19.3$ MeV ($E =$ 11.3 MeV). Instead, the cruder expression (7) exceeds

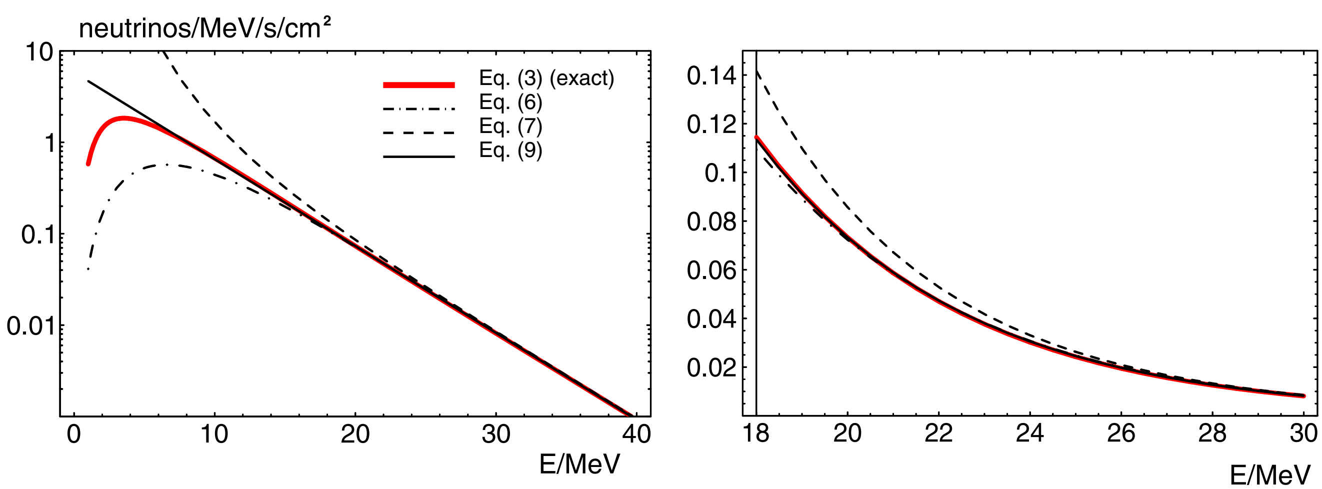

FIG. 2 (color online). An illustration of the approximate analytical descriptions of the DSNνF spectrum in comparison with the exact spectrum calculated numerically (details in the legend). The lower panel is a close-up of the upper one on a linear scale. I used the same SNR parameters and luminosity as in Fig. 1 and the spectral parameters $E_0 = 15$ MeV, $\alpha = 2.6$. For the fitted exponential form, Eq. (9), the value of the characteristic energy is $\langle E\rangle = 4.57$ MeV.

the exact result by up to 40% at $E = 19.3$ and up to a factor of 3 at $E = 11.3$ MeV.

The analytical results lose accuracy for larger β, as expected, since larger β means larger contribution of supernovae at $z > 1$. With $\beta = 5$, the sophisticated result (6) errs by up to 20% (120%) at $E = 19.3$ MeV ($E = 11.3$ MeV). Equation (7) can deviate from the exact result by a factor of several.

The exponential form, Eq. (9), with $\langle E \rangle$ fitted to reproduce the exact result at $E \sim 20$–30 MeV, is accurate within 5% everywhere above 20 MeV and deviates from the exact spectrum by at most 25% at $E = 11.3$ MeV.

In closing this section, I would like to emphasize that, while it useful for understanding, the analytical approximations discussed here lose validity below 15–20 MeV of energy. Thus, to model observables at these low energies, it is necessary to calculate the neutrino flux numerically using Eq. (1). I do so in the remainder of this work.

IV. DETECTING THE DIFFUSE FLUX: OBSERVABLES

A. Inverse beta decay: signal and background

I now turn to the spectrum of events induced by the diffuse flux in a detector. In particular, I consider events due to inverse beta decay, $\bar{\nu}_e + p \rightarrow n + e^+$, since they largely dominate the signal in water and in liquid scintillator.

The detected positrons from inverse beta decay carry information on the incoming $\bar{\nu}_e$ spectrum. This is thanks to the fact that, except for small effects due to nucleon recoil, the neutrino and positron energy differ simply by the mass difference of the neutron and proton: $E_{e^+} = E - 1.29$ MeV. Thus, the positron energy spectrum is roughly given by the neutrino spectrum distorted by the energy dependence of the detection cross section, which goes approximately as E^2.

To calculate the spectrum of the observed positrons, I model the diffuse $\bar{\nu}_e$ flux according to Eq. (1), with $z_{max} = 5$. In all cases, I will use the typical values $R_{SN}(0) = 10^{-4}\ \mathrm{Mpc}^{-3}\,\mathrm{yr}^{-1}$ and $L = 5 \times 10^{52}$ ergs, and vary α, E_0, and β in the intervals that I indicated as typical in Sec. II. I use the detection cross section from Ref. [28].

For definiteness, results are given for a water Cherenkov detector of 0.45 Mton fiducial volume (20 times the volume of SK) without and with gadolinium, after 4 years of operation. I consider two different energy thresholds, 18 MeV and 10 MeV in positron energy, characteristic of water only and water with gadolinium (water + Gd hereafter), respectively. I adopt the same energy resolution and efficiency ($\simeq 93\%$ in the energy range relevant here [29]) as SK [30,31]. The setups considered here are the same as those in Ref. [16] (except for a minor difference in the volume: 0.4 Mton in Ref. [16] and 0.45 Mton in this work), so that a direct comparison is possible.

For a meaningful interpretation of the results, it is necessary to carefully take into account the background. As described in a number of publications (e.g., [24] and references therein), there are four sources of background that in water are truly ineliminable. These are spallation neutrons, reactor neutrinos, atmospheric neutrinos, and invisible muons. The first one is dealt with by setting the energy threshold at 18 MeV of positron energy. Above this cut the spallation and reactor backgrounds are practically zero. The remaining backgrounds, atmospheric neutrinos and invisible muons, can only be included in the statistical analysis, as done in [3], so that the signal and these backgrounds can be separated only on a statistical basis. Of these, the invisible muon background is larger than the DSNνF signal by a factor of several [3,16].

The addition of gadolinium to the water will allow us to discriminate inverse beta decay events from events of other types, thanks to the detection in coincidence of the positron and of the neutron capture on Gd [7]. With Gd, the energy threshold can be lowered to 10 MeV of positron energy, motivated by the presence of the reactor $\bar{\nu}_e$'s below it. It is estimated that in the water + Gd configuration the invisible muon background will be reduced by a factor of $\sim$5 with respect to pure water [8]. This reduction will bring it down to be smaller or comparable to the signal above the 10 MeV threshold.

Here I model the background following Ref. [16]. As done there, the events due to background will not be shown, but will be included in the calculation of the statistical error. More explicitly, I consider a scenario in which from the total of the data one subtracts the background using a Monte Carlo prediction for it. The error on the subtracted signal is then given by the statistical error on the total (signal plus background) number of events: $\sigma = \sqrt{N_{sig} + N_{bkg}}$.

The results of this work can be easily rescaled to reproduce the inverse beta decay signal at other detectors (up to differences due to different energy resolution). The case of the proposed 50 kt liquid scintillator detector LENA [12,13] is particularly interesting. Since a scintillator distinguishes inverse beta decay through the detection of the positron and neutron in coincidence, its performance will be similar to that of a water + Gd detector, up to a rescaling to account for the different volume. I estimate that, in terms of number of events, 1 (4) year(s) of running time of a 0.45 Mton water + Gd detector with the efficiency given above corresponds to $\sim$7.4 ($\sim$ 30) years running time of LENA with 100% efficiency. Equivalently, for the same running time, LENA will have a number of events smaller by a factor $\sim$0.13.

B. The positron energy spectrum

Figures 3 and 4 give the spectra of events in 5 MeV bins for the water-only configuration and the water + Gd one. For visual convenience, in each figure all the histograms

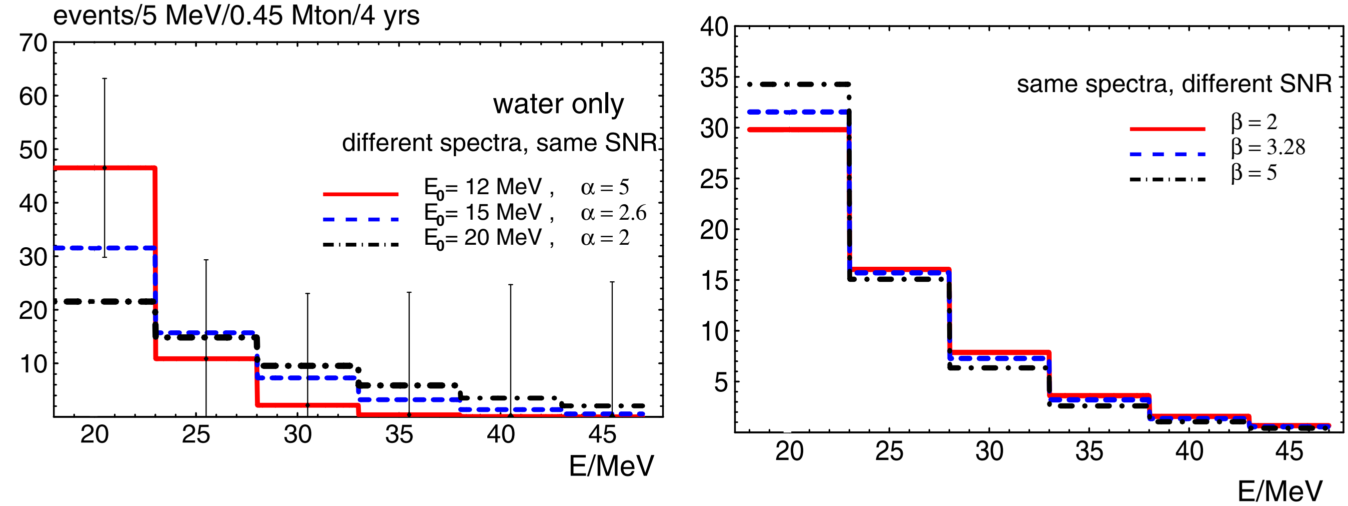

FIG. 3 (color online). The spectra of the observed positrons from inverse beta decay for the pure water setup, for fixed SNR (upper panel, $\beta = 3.28$ used), and for the fixed original neutrino spectrum (lower panel, $E_0 = 15$ MeV, $\alpha = 2.6$ used). In all cases the numbers of events have been normalized to $N = 60$.

have been normalized at the same number of events, $N = 60$ for water only and $N = 150$ for water + Gd. These are the numbers obtained with $\alpha = 2.6$, $E_0 = 15$ MeV, and $\beta = 3.28$. Each figure has two panels: in the upper one I fix the cosmology and vary the neutrino spectral parameters, α and E_0, while in the lower panel the spectral parameters are fixed and β is varied (see figure captions for details). The error bars (omitted in the lower panel for simplicity) represent the 1σ *total* (signal + background) statistical errors.

Let us first comment on the water-only case, Fig. 3. It appears immediately that the spectrum changes substantially when the spectral parameters are varied. The behavior agrees with what was expected from Sec. III: the spectrum falls more rapidly for the smaller ϵ, according to the exponential dependence in the DSNνF spectrum. So, a first conclusion is that, in principle, the signal induced by the diffuse flux is very sensitive to the original neutrino spectrum.

In spite of this, however, different DSNνF spectra—and therefore different original spectra—will be difficult to distinguish one from the other with high statistical confidence. This appears from the error bars plotted in Fig. 3. One can see that the largest variation of the numbers of events in the first bin is within 2σ statistical error, and the variations are smaller in the other energy bins. As already anticipated in [16], this means that with typical statistics a Megaton water detector would be able to give indication or evidence of the DSNνF, but would not be able to give precise spectral information about it. With higher DSNνF flux—within what is allowed by the current SK limit—the spectral sensitivity could be moderately better. For example, with twice as many signal events, the variation of

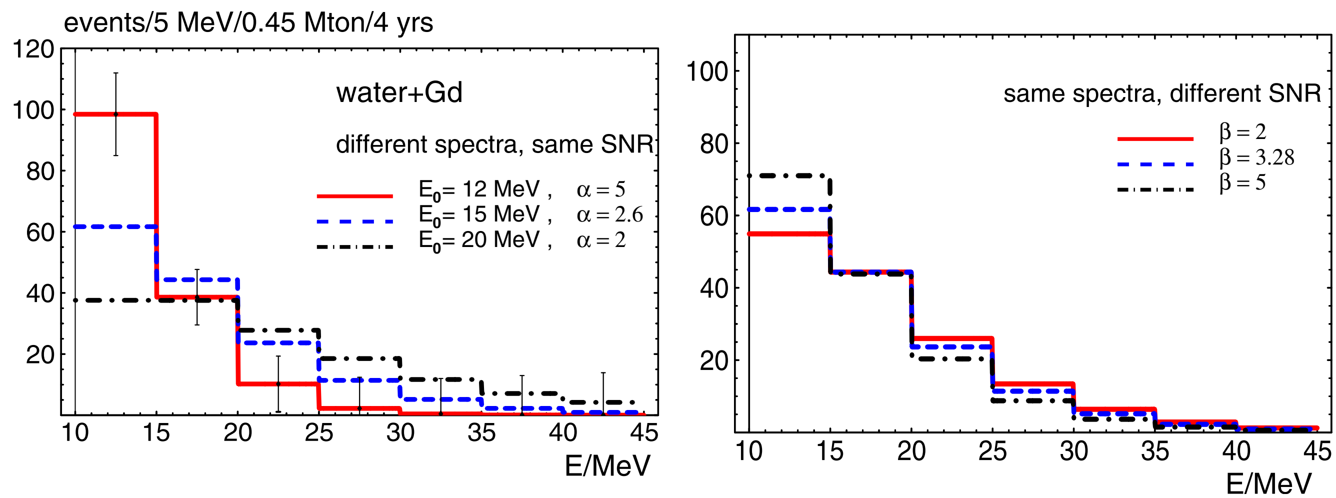

FIG. 4 (color online). Same as Fig. 3 for water + Gd. The numbers of events have been normalized to $N = 150$ in all cases.

signal between the two extreme cases in the first energy bin would be of about $\sim 3\sigma$. Notice that the total statistical error is dominated by the invisible muon background and therefore would increase only weakly with the increase of the signal.

The lower panel of Fig. 3 confirms the expectation of little dependence on the SNR parameter β. Even with the rather extreme variations of β used in the figure, the number of events varies by at most $\sim 15\%$ in the bins where the statistics is higher. Considering the large errors, I conclude that very little or no information on β could be extracted from DSNνF data.

With water + Gd the potential to study the DSNνF spectrum is dramatically better: indeed, the statistical errors are smaller thanks to the improved background reduction, and the signal is enhanced by the lower energy threshold. Figure 4 illustrates this. It appears that the two extreme cases differ by more than 3σ in the first bin. This means that the possibility of spectrum discrimination is concrete, even though the differences in the other bins are not as significant. As in the case of pure water, the dependence of the observed spectrum on β is weak. The difference between the number of events in the first bin for the two extreme scenarios is at the level of $\sim 1\sigma$, increasing to $\sim(2\text{–}2.5)\sigma$ for a doubled or tripled signal. Thus, to discriminate between different values of β would be difficult, even in the ideal case of the perfectly known original spectrum.

The points made above can be illustrated more quantitatively using the ratio r of the number of events in the first and second energy bins. Taking bins of 5 MeV width, this ratio is

$$r \equiv \frac{N(18 \leq E_{e^+}/\mathrm{MeV} < 23)}{N(23 \leq E_{e^+}/\mathrm{MeV} < 28)}, \tag{10}$$

for the water-only case, and

$$r \equiv \frac{N(10 \leq E_{e^+}/\mathrm{MeV} < 15)}{N(15 \leq E_{e^+}/\mathrm{MeV} < 20)}, \tag{11}$$

for water + Gd, in terms of the positron energy E_{e^+}. To limit oneself to the numbers of events in the first two bins is overall more convenient with respect to including the data in the higher energy bins. The latter add little to the signal but add substantially to the background, and therefore they end up washing out the effect of the signal by increasing the error.

For pure water and fixed SNR (Fig. 3, upper panel) I find that r varies in the range $r \simeq 1.5\text{–}4.3$. With the statistics used in Fig. 3, the error on r is larger than $\sim 100\%$; this confirms the conclusion that the sensitivity to the neutrino spectrum is limited. For the fixed original spectrum and varying β, the variation of r is minimal, much smaller than the error.

For the water + Gd configuration in the case of fixed SNR (Fig. 4, upper panel), I have $r \simeq 1\text{–}2.5$. The error is $\sim 20\%\text{–}30\%$, meaning that at least the extreme cases should be distinguishable for typical luminosity of the DSNνF. For the fixed original spectrum and varying β, I get $r \simeq 1.2\text{–}1.6$, which is smaller than the error unless the DSNνF is close to the SK upper limit.

C. Number of events

To complement the study of the DSNνF spectrum—which is the main focus of this paper—here I give a brief discussion of the event rates and their information content.

As it is clear from the previous sections, the number of events in a detector depends on the original neutrino spectrum, on the SNR power β, and on the overall factors $R_{\mathrm{SN}}(0)$ and L, i.e. the normalization of the SNR and the neutrino luminosity in $\bar{\nu}_e$ (after oscillations). Once the detection of the DSNνF moves from the discovery to the precision phase, the event rate will constrain the product $R_{\mathrm{SN}}(0) \times L$ and will complement the spectral analysis to extract E_0, α, and β. Realistically, these two aspects cannot be separated: the data will be analyzed by a global fit with both the spectral parameters and the overall factors as fit variables. Still, for illustration it is useful to discuss certain limiting cases where the sensitivity to the overall factors and that to the spectral parameters can be treated separately.

If the DSNνF spectrum is reconstructed very precisely by the spectral analysis, the event rate will serve mainly to constrain $R_{\mathrm{SN}}(0) \times L$. This can happen for the water + Gd setup, where the statistical errors are small enough to allow spectral reconstruction. High precision would be obtained if the DSNνF signal is particularly luminous, typically 2 or more times larger than in Fig. 4. In the ideal case of the perfectly known spectrum, the error on the $R_{\mathrm{SN}}(0) \times L$ inferred from the data would be just the statistical error, of the order of tens of percent. This would be an enormous improvement with respect to the current information from supernova observations [which constrain $R_{\mathrm{SN}}(0)$] and from the neutrino data from SN1987A (see e.g. [21]).

It should be considered that, by the time the DSNνF is detected, the SNR could be better known from new supernova surveys like JWST [32] and SNAP [33], since these are expected to see thousands of core collapse supernovae while undertaking their primary mission of observing type Ia supernovae. From these surveys we are likely to obtain a precise measurement of β, while some systematic uncertainty on $R_{\mathrm{SN}}(0)$ will be left due to extinction effects. In this situation, the measured β will be used as input in the DSNνF spectral analysis, thus increasing the precision of reconstruction of E_0 and α. The astrophysical measurement of $R_{\mathrm{SN}}(0)$ and the information on $R_{\mathrm{SN}}(0) \times L$ from the neutrino event rate will be combined to constrain L and reduce the systematic error on $R_{\mathrm{SN}}(0)$. If the systematics due to extinction is well understood and taken into account, the DSNνF event rate will essentially measure L.

It is possible that the product $R_{SN}(0) \times L$ and the power β will be much better known than the original neutrino spectrum. This scenario could be realized if $R_{SN}(0)$ and β are precisely measured by supernova surveys (plus precise treatment of systematic effects) and L is determined by improved numerical simulations of core collapse, perhaps combined with astrophysical data on supernovae such as energy of the explosion, mass of the remnant, etc.

In this case the event rate will serve to constrain the spectral parameters in combination with the energy distribution of the data. In Fig. 5 I briefly illustrate this scenario in the ideal situation in which L, $R_{SN}(0)$, and β are known with negligible error (see caption for details). The figure shows isocontours of the ratio r and of the event rate N in the plane $\alpha - E_0$, both for water only and for water with gadolinium. It appears that the event rate varies by a factor of several depending on the spectral parameters: from $\sim$10 to $\sim$140 ($\sim$70–230) events in 4 years for water only (water plus gadolinium) [34]. The figure also illustrates a possible measurement of N and r, with central values and 1σ statistical errors on these two quantities [35]. If only r is considered—for robustness against uncertainties on $R_{SN}(0) \times L$—then for water only a major portion of the parameter space is allowed within 1σ, and the entire space is within 3σ. Instead, for water + Gd the 1σ allowed region is much more restricted, and the 3σ region excludes the edges of the parameter space; for example, the measurement of $r = 1.2$ would exclude the point $E_0 = 12$ MeV and $\alpha = 4.5$. Including the information on the number of events reduces the allowed region substantially: while for pure water the whole $\alpha - E_0$ plane is allowed within 3σ, for water + Gd the potential for exclusion is better. For the specific case in the figure, a measurement of $N = 200$ would exclude $E_0 = 12$ MeV regardless of the value of α.

Notice that the region allowed by N is contained inside the one allowed by r, meaning that the number of events alone is sufficient to constrain the original neutrino spectrum, if L, $R_{SN}(0)$, and β are known very precisely. In the presence of errors on these quantities, which is probably more realistic, the ratio r will be more constraining instead.

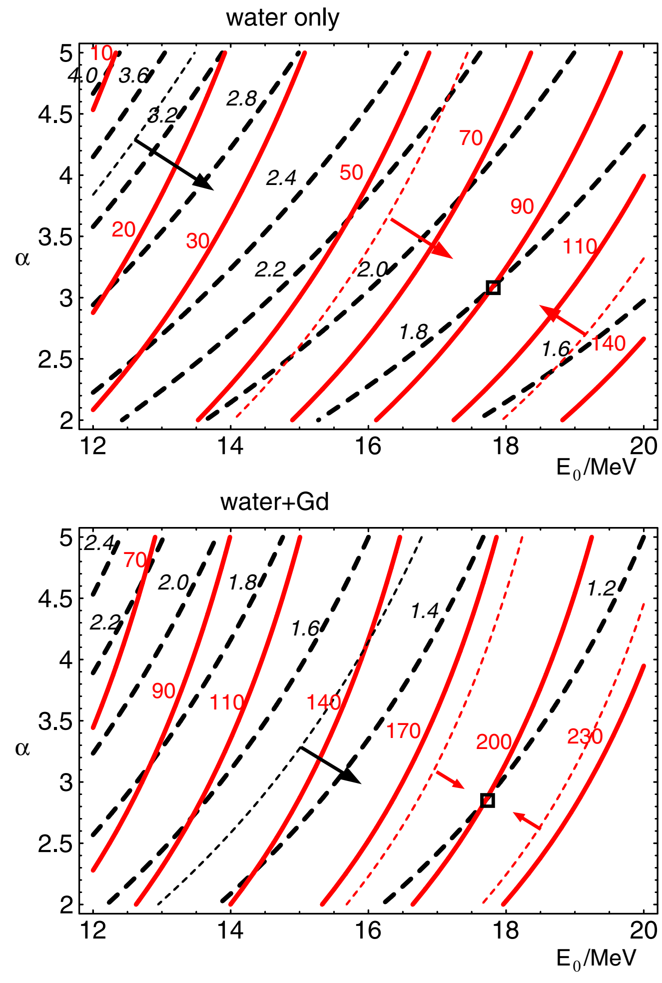

FIG. 5 (color online). Solid (red) lines: isocontours of the number of events in 4 years running time, N, in the space $\alpha - E_0$. Long dashed (black) lines: isocontours of the ratio r of the numbers of events in the first and second bins [Eqs. (10) and (11)]. In each panel I show a possible measurement of N and r, with central values (diamond) and 1σ statistical errors (regions within the short dashed lines, marked with arrows; the wider region is the error on r). The SNR parameters and luminosity are as in Fig. 1.

V. SUMMARY AND DISCUSSION

It is a concrete possibility that the next supernova neutrino data will be from the diffuse flux. If so, these data will be of interest to improve on our knowledge of the supernova neutrino spectrum with respect to what is already known from SN1987A. Furthermore, the DSNνF data will be analyzed to test the cosmological rate of supernovae.

Here I have addressed the question of the sensitivity of the DSNνF to these quantities, both at the level of the $\bar{\nu}_e$ flux at Earth and of the spectrum of inverse beta decay events in a detector.

A first answer is that the spectrum of the diffuse $\bar{\nu}_e$ at Earth above realistic detection thresholds (10 MeV or higher) essentially reflects the neutrino spectrum at the source (after oscillations), with only a weak (tens of percent) dependence on the power β of evolution of the supernova rate with the redshift. Indeed, with respect to the original spectrum, the DSNνF spectrum retains the same structure of an exponential times a polynomial part. The exponential term is identical to the one in the original spectrum, and dominates the energy dependence of the DSNνF spectrum. The information on the cosmology is in the coefficients of the polynomial, and therefore the cosmological parameters influence the spectrum more weakly. These features, that were studied in detail here, are in agreement with the general intuition about the contribution of more distant supernovae being weak at high energy due to the redshift.

At the level of experiment, a better background subtraction with respect to pure water [e.g., by the addition of gadolinium to the water of UNO/HyperKamiokande/MEMPHYS or by using a large scintillator detector (LENA)] would be needed to move from the discovery phase to the precision phase.

What major advances will come from the precision phase depends on the situation in the field at that time. A likely scenario is that there will be new, precise measurements of the supernova rate. These will result in a precise determination of β, while leaving some uncertainty on the overall scale of the SNR, $R_{SN}(0)$, due to effects of extinction. In this case, the DSNνF data will mainly improve our knowledge of the original neutrino spectrum, thus adding precious information to what is already known from SN1987A. For typical luminosity of the signal, after 4 years of operation a 0.45 Mton detector in the water + Gd configuration would have hundreds of signal events, and total (signal + background) statistical error of $\sim$10%–30% in the first two energy bins. This should make it possible to discriminate at least between the extreme cases of the neutrino spectrum.

In addition to the spectrum, the observation of the DSNνF will allow us to measure the product of the neutrino luminosity and of $R_{SN}(0)$. This measurement will be combined with direct supernova observations to reduce the uncertainty on $R_{SN}(0)$.

In the exciting case in which data from a new galactic supernova become available before the DSNνF is measured, the study of the DSNνF will take a completely different direction. The high statistics data from the galactic supernova will give the neutrino spectrum and luminosity with very good precision. These and the value of β from supernova surveys will be used as input in the analysis of the DSNνF to extract information on the less precise parameter $R_{SN}(0)$.

Depending on the precision on the DSNνF signal, a number of interesting tests could be performed. One of them is to look for differences between the value of $R_{SN}(0)$ estimated in astronomy and the one obtained from neutrinos: the comparison could reveal a number of "failed" supernovae—objects that undergo core collapse with the emission of neutrinos without a visible explosion. It would also be interesting to look for differences between the neutrino spectrum inferred from an individual galactic supernova and the one extracted from the DSNνF: such differences will be a measure of the variation of the neutrino output from one supernova to another. Differences could be expected in consideration of the fact that the DSNνF receives the largest contribution from low mass supernovae, $M \sim 8$–$10 M_{\odot}$ (simply because the initial mass function goes roughly like the power -2 of the star's mass; see e.g. [22] and references therein), whose neutrino output could differ from that of a supernova with a larger mass progenitor.

In summary, the present study shows the relevance of studying the energy spectrum of the diffuse supernova neutrino flux, mainly as a tool to reconstruct the original neutrino spectrum and therefore to test the physics of core collapse that influences the neutrino spectrum formation inside the star. It also motivates the experimental effort to reduce the background in the relevant energy window in order to achieve the necessary precision for spectral sensitivity.

ACKNOWLEDGMENTS

I acknowledge support from the INT-SCiDAC Grant No. DE-FC02-01ER41187.

[1] N. Arnaud *et al.*, Astropart. Phys. **21**, 201 (2004).
[2] S. Ando, J. F. Beacom, and H. Yuksel, Phys. Rev. Lett. **95**, 171101 (2005).
[3] M. Malek *et al.* (Super-Kamiokande), Phys. Rev. Lett. **90**, 061101 (2003).
[4] K. Eguchi *et al.* (KamLAND), Phys. Rev. Lett. **92**, 071301 (2004).
[5] C. Lunardini, Phys. Rev. D **73**, 083009 (2006).
[6] B. Aharmim *et al.* (SNO), Astrophys. J. **653**, 1545 (2006).
[7] J. F. Beacom and M. R. Vagins, Phys. Rev. Lett. **93**, 171101 (2004).
[8] H. Yuksel, S. Ando, and J. F. Beacom, Phys. Rev. C **74**, 015803 (2006).
[9] K. Nakamura, Int. J. Mod. Phys. A **18**, 4053 (2003).
[10] C. K. Jung, AIP Conf. Proc. **533**, 29 (2000).
[11] L. Mosca, Nucl. Phys. B, Proc. Suppl. **138**, 203 (2005).
[12] T. Marrodan Undagoitia *et al.*, Prog. Part. Nucl. Phys. **57**, 283 (2006).
[13] M. Wurm *et al.*, Phys. Rev. D **75**, 023007 (2007).
[14] A. Ereditato and A. Rubbia, Nucl. Phys. B, Proc. Suppl. **155**, 233 (2006).
[15] D. B. Cline, F. Raffaelli, and F. Sergiampietri, JINST **1**, T09001 (2006).
[16] G. L. Fogli, E. Lisi, A. Mirizzi, and D. Montanino, J. Cosmol. Astropart. Phys. 04 (2005) 002.
[17] A. S. Dighe and A. Y. Smirnov, Phys. Rev. D **62**, 033007 (2000).
[18] C. Lunardini and A. Y. Smirnov, J. Cosmol. Astropart. Phys. 06 (2003) 009.
[19] M. T. Keil, G. G. Raffelt, and H.-T. Janka, Astrophys. J. **590**, 971 (2003).
[20] In [21] it was pointed out that a spectrum of the type (1) misses certain spectral shapes that also fit the SN1987A data well. Those match Eq. (1), however, above the

average energy of the spectrum, which is the regime of interest here.
[21] C. Lunardini, Astropart. Phys. **26**, 190 (2006).
[22] A. M. Hopkins and J. F. Beacom, Astrophys. J. **651**, 142 (2006).
[23] L. Hernquist and V. Springel, Mon. Not. R. Astron. Soc. **341**, 1253 (2003).
[24] S. Ando and K. Sato, New J. Phys. **6**, 170 (2004).
[25] Basic physics arguments as well as numerical models indicate that the main features of a supernova neutrino burst are fairly universal, with only little dependence on the progenitor mass. However some dependence, at the level of ten percent or so, in the average energy and luminosities is expected in the neutrino emission during the accretion phase, and has been seen in the output of numerical codes; see e.g. [36,37].
[26] I recall the expressions of the function Γ: $\int dx x^w e^{-x} = -\Gamma(w+1, x)$, $\Gamma(n+1, x) = n! e^{-x} \sum_{k=0}^{n} \frac{x^k}{k!}$, the second being valid only for integer n.
[27] M. S. Malek, Ph.D thesis, State University of New York at Stony Brook (Report No. UMI-31-06530, 2003), available at http://www-sk.icrr.u-tokyo.ac.jp/sk/index-e.html.
[28] A. Strumia and F. Vissani, Phys. Lett. B **564**, 42 (2003).
[29] In the SK analysis [27] several experimental cuts reduced the efficiency down to 47% (79%) below (above) 34 MeV. This could change in the future depending on the details of the data processing. Thus, for the sake of generality here I consider the generic instrumental efficiency of the SK detector.
[30] K. S. Hirata *et al.*, Phys. Rev. D **38**, 448 (1988).
[31] J. N. Bahcall, P. I. Krastev, and E. Lisi, Phys. Rev. C **55**, 494 (1997).
[32] JWST web page, http://www.jwst.nasa.gov.
[33] SNAP letter of intent, available at http://snap.lbl.gov.
[34] These event rates are well compatible with the current upper limit from Super-Kamiokande [3]. Such a limit allows up to 3.5 events/year at SK [27], corresponding to about 250 events in 4 years in a 0.45 Mton detector in the water-only configuration.
[35] For the number of events, I have used the sum of the numbers of events in the first three (four) energy bins for pure water (water + Gd). The higher energy bins are background dominated and thus including them would increase the error on the signal.
[36] M. Liebendoerfer *et al.*, Nucl. Phys. **A719**, C144 (2003).
[37] F. S. Kitaura, H.-T. Janka, and W. Hillebrandt, astro-ph/0512065.